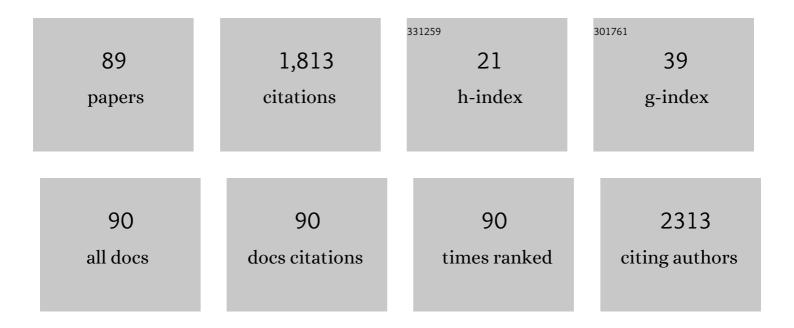
Choong Kyun Rhee

List of Publications by Year in descending order

Source: https://exaly.com/author-pdf/4522550/publications.pdf Version: 2024-02-01



#	Article	IF	CITATIONS
1	Increased Electrocatalyzed Performance through Dendrimer-Encapsulated Gold Nanoparticles and Carbon Nanotube-Assisted Multiple Bienzymatic Labels: Highly Sensitive Electrochemical Immunosensor for Protein Detection. Analytical Chemistry, 2013, 85, 1784-1791.	3.2	169
2	Amplified Electrochemical Detection of a Cancer Biomarker by Enhanced Precipitation Using Horseradish Peroxidase Attached on Carbon Nanotubes. Analytical Chemistry, 2012, 84, 6407-6415.	3.2	168
3	Electrochemical Capacitances of Well-Defined Carbon Surfaces. Langmuir, 2006, 22, 9086-9088.	1.6	104
4	Size Effect of Pt Nanoparticle on Catalytic Activity in Oxidation of Methanol and Formic Acid: Comparison to Pt(111), Pt(100), and Polycrystalline Pt Electrodes. Langmuir, 2009, 25, 7140-7147.	1.6	102
5	Highly graphitized carbon from non-graphitizable raw material and its formation mechanism based on domain theory. Carbon, 2017, 121, 301-308.	5.4	68
6	Electrocatalytic Oxidation of Formic Acid and Methanol on Pt Deposits on Au(111). Langmuir, 2007, 23, 10831-10836.	1.6	66
7	Bi-modified Pt supported on carbon black as electro-oxidation catalyst for 300 W formic acid fuel cell stack. Applied Catalysis B: Environmental, 2019, 253, 187-195.	10.8	60
8	Atomic and Molecular Adsorption on the Bi(111) Surface: Insights into Catalytic CO ₂ Reduction. Journal of Physical Chemistry C, 2018, 122, 23084-23090.	1.5	48
9	Modification of Pt nanoelectrodes dispersed on carbon support using irreversible adsorption of Bi to enhance formic acid oxidation. Electrochimica Acta, 2008, 53, 7744-7750.	2.6	46
10	A highly sensitive quartz crystal microbalance immunosensor based on magnetic bead-supported bienzymes catalyzed mass enhancement strategy. Biosensors and Bioelectronics, 2015, 66, 539-546.	5.3	45
11	Photocatalytic CO2 reduction and hydrogen production over Pt/Zn-embedded β-Ga2O3 nanorods. Applied Surface Science, 2021, 536, 147753.	3.1	41
12	Impedance Analysis for Hydrogen Adsorption Pseudocapacitance and Electrochemically Active Surface Area of Pt Electrode. Langmuir, 2009, 25, 11947-11954.	1.6	31
13	Sensitivity enhancement of an electrochemical immunosensor through the electrocatalysis of magnetic bead-supported non-enzymatic labels. Biosensors and Bioelectronics, 2014, 54, 351-357.	5.3	31
14	A stable and sensitive voltammetric immunosensor based on a new non-enzymatic label. Biosensors and Bioelectronics, 2013, 50, 118-124.	5.3	30
15	Two electrochemical processes for the deposition of Sb on Au(100) and Au(111): irreversible adsorption and underpotential deposition. Journal of Electroanalytical Chemistry, 1997, 436, 277-280.	1.9	29
16	Modification of Au Nanoparticles Dispersed on Carbon Support Using Spontaneous Deposition of Pt toward Formic Acid Oxidation. Langmuir, 2010, 26, 4497-4505.	1.6	29
17	Formic acid electrooxidation activity of Pt and Pt/Au catalysts: Effects of surface physical properties and irreversible adsorption of Bi. Electrochimica Acta, 2018, 273, 307-317.	2.6	28
18	Photocatalytic and photoelectrocatalytic properties of Eu(III)-doped perovskite SrTiO3 nanoparticles with dopant level approaches. Materials Science in Semiconductor Processing, 2021, 132, 105919.	1.9	28

#	Article	IF	CITATIONS
19	Simultaneous determination of nonionic and anionic industrial surfactants by liquid chromatography combined with evaporative light-scattering detection. Journal of Chromatography A, 2004, 1046, 289-291.	1.8	27
20	Simultaneous separation of nine surfactants of various types by HPLC with evaporative light scattering detection. Talanta, 2006, 70, 481-484.	2.9	26
21	Fe nanoparticle entrained in tubular carbon nanofiber as an effective electrode material for metal–air batteries: A fundamental reason. Carbon, 2014, 80, 698-707.	5.4	24
22	Contrasting electrochemical behavior of irreversibly adsorbed Sb monolayer on Pt(100) and Pt(111) single crystal electrode surfaces. Journal of Electroanalytical Chemistry, 1998, 453, 243-247.	1.9	21
23	Ensemble size estimation in formic acid oxidation on Bi-modified Pt(111). Electrochemistry Communications, 2010, 12, 1731-1733.	2.3	20
24	Photoelectrochemical Hydrogen Evolution and CO2 Reduction over MoS2/Si and MoSe2/Si Nanostructures by Combined Photoelectrochemical Deposition and Rapid-Thermal Annealing Process. Catalysts, 2019, 9, 494.	1.6	19
25	Electrochemical hydrogen evolution and CO2 reduction over hierarchical MoSxSe2-x hybrid nanostructures. Applied Surface Science, 2019, 489, 976-982.	3.1	19
26	Photoluminescence, electro- and thermal catalytic properties of bare and Eu(III)-doped GaOOH, α- and β-Ga2O3 nanorods. Journal of Alloys and Compounds, 2019, 774, 11-17.	2.8	19
27	Electrochemical Atomic Layer Processing. Materials and Manufacturing Processes, 1995, 10, 283-301.	2.7	18
28	Electrochemical Scanning Tunneling Microscopic Observation of the Preoxidation Process of CO on Pt(111) Electrode Surface. Langmuir, 2007, 23, 9495-9500.	1.6	18
29	Effects of oxidation and heat treatment of acetylene blacks on their electrochemical double layer capacitances. Carbon, 2009, 47, 226-233.	5.4	17
30	Pt Deposits on Bi/Pt NP Catalyst for Formic Acid Oxidation: Catalytic Enhancement and Longer Lifetime. Langmuir, 2020, 36, 5359-5368.	1.6	17
31	Simultaneous determination of nonionic and anionic industrial surfactants by liquid chromatography combined with evaporative light-scattering detection. Journal of Chromatography A, 2004, 1046, 289-291.	1.8	17
32	Formic acid oxidation on Bi-modified Pt surfaces: Pt deposits on Au versus bulk Pt. Electrochimica Acta, 2016, 216, 16-23.	2.6	16
33	Paramagnetic Ho2O3 nanowires, nano-square sheets, and nanoplates. Ceramics International, 2018, 44, 17919-17924.	2.3	16
34	Electrochemical Recovery and Behaviors of Rare Earth (La, Ce, Pr, Nd, Sm, Eu, Gd, Tb, Dy, Ho, Er, Tm, and) Tj ETQ	q0 0 0 rgE	BT /Overlock 1

35	CO2 reduction by photocatalytic and photoelectrocatalytic approaches over Eu(III)-ZnGa2O4 nanoparticles and Eu(III)-ZnGa2O4/ZnO nanorods. Journal of CO2 Utilization, 2022, 60, 101994.	3.3	16
36	Initial adsorption stage of irreversibly adsorbing Sb on Au(111). Journal of Electroanalytical Chemistry, 2004, 566, 1-5.	1.9	15

CHOONG KYUN RHEE

#	Article	IF	CITATIONS
37	Photoelectrochemical and photocatalytic detoxification of Cr(VI) to Cr(III) over terpyridine-derivatized Au nanoparticles on carbon paper and indium-tin-oxide electrodes. Chemical Engineering Journal, 2020, 402, 126266.	6.6	14
38	Electrodeposition and Characterization of Lanthanide Elements on Carbon Sheets. Coatings, 2021, 11, 100.	1.2	14
39	Electrochemical scanning tunneling microscope study of irreversibly adsorbed Te on a Pt(111) single crystal electrode surface. Journal of Electroanalytical Chemistry, 2001, 506, 149-154.	1.9	13
40	Contrasting Electrochemical Behavior of CO, Hydrogen, and Ethanol on Single-Layered and Multiple-Layered Pt Islands on Au Surfaces. Journal of Physical Chemistry C, 2014, 118, 24425-24436.	1.5	13
41	Structural evolution of irreversibly adsorbed Bi on Pt(111) under potential excursion. Journal of Solid State Electrochemistry, 2013, 17, 3109-3114.	1.2	12
42	Formation of Single-Layered Pt Islands on Au(111) Using Irreversible Adsorption of Pt and Selective Adsorption of CO to Pt. Langmuir, 2014, 30, 4203-4206.	1.6	12
43	Electrochemical Eu(iii) behaviours and Eu oxysulfate recovery over terpyridine-functionalized indium tin oxide electrodes. Inorganic Chemistry Frontiers, 2021, 8, 1175-1188.	3.0	12
44	Morphological reason for enhancement of electrochemical double layer capacitances of various acetylene blacks by electrochemical polarization. Electrochimica Acta, 2008, 53, 5789-5795.	2.6	11
45	Electrochemical Ce(III)/Ce(IV) Redox Behavior and Ce Oxide Nanostructure Recovery over Thio-Terpyridine-Functionalized Au/Carbon Paper Electrodes. ACS Applied Materials & Interfaces, 2021, 13, 27594-27611.	4.0	11
46	Atomic Rearrangements during the Electrochemical Treatments of Au(111) Covered with Irreversibly Adsorbed Sb. Journal of Physical Chemistry B, 2005, 109, 8961-8966.	1.2	10
47	ToF-SIMS imaging and spectroscopic analyses of PEG-conjugated AuNPs. Surface and Interface Analysis, 2011, 43, 628-631.	0.8	10
48	Conical multiple-layered Pt deposits on Au and its adsorption stoichiometries of CO and hydrogen. Electrochimica Acta, 2018, 290, 244-254.	2.6	10
49	Co oxidation on LaCoO3 perovskite. Korean Journal of Chemical Engineering, 1994, 11, 48-54.	1.2	9
50	2-Dimensional atomic arrangements of Te on Pt(111) whose coverage is higher than 0.25+. Journal of Solid State Electrochemistry, 2005, 9, 247-253.	1.2	9
51	Oxygen reduction on composite FeOx nanoparticles embedded in porous carbon. Electrochimica Acta, 2011, 58, 422-426.	2.6	9
52	Assembly of strands of multiwall carbon nanotubes and gold nanoparticles using alkanedithiols. Carbon, 2011, 49, 487-494.	5.4	9
53	Formic acid oxidation on Pt deposit model catalysts on Au: Single-layered Pt deposits, plateau-type Pt deposits, and conical Pt deposits. Electrochimica Acta, 2019, 310, 38-44.	2.6	9
54	Photocatalytic CO2 Reduction and Electrocatalytic H2 Evolution over Pt(0,II,IV)-Loaded Oxidized Ti Sheets. Nanomaterials, 2020, 10, 1909.	1.9	9

CHOONG KYUN RHEE

#	Article	IF	CITATIONS
55	Structural evolution of self-assembled monolayer of 1-mercapto-2-propanol on Au(111) in a N2 flow: an electrochemical and STM study. Applied Surface Science, 2004, 228, 313-319.	3.1	8
56	Electrochemical STM observation of new structures of CO adsorbed on a Pt(111) electrode surface. Chemical Communications, 2006, , 2191.	2.2	8
57	Electrochemical Eu(III)/Eu(II) behaviors and recovery over terpyridyl-derivatized modified indium tin oxide electrode surfaces. Chemical Engineering Journal, 2021, 412, 128717.	6.6	8
58	CO preoxidation on Ru-modified Pt(111). Electrochemistry Communications, 2010, 12, 1363-1366.	2.3	7
59	Selective adsorption of dithiolate-modified multi-wall carbon nanotubes onto alkanethiol self-assembled monolayers on Au(111). Chemical Communications, 2010, 46, 6584.	2.2	7
60	Structure and electrochemical applications of boron-doped graphitized carbon nanofibers. Nanotechnology, 2012, 23, 315602.	1.3	7
61	Quantitative analysis of BF4a^' ions infiltrated into micropores of activated carbon fibers using nuclear magnetic resonance. RSC Advances, 2014, 4, 16726.	1.7	7
62	Irreversibly Adsorbed Tri-metallic PtBiPd/C Electrocatalyst for the Efficient Formic Acid Oxidation Reaction. Journal of Electrochemical Science and Technology, 2020, 11, 84-91.	0.9	7
63	Electrochemical Ce3+/Ce4+ and Eu2+/Eu3+ interconversion, complexation, and electrochemical CO2 reduction on thio-terpyridyl-derivatized Au electrodes. Applied Surface Science, 2022, 576, 151793.	3.1	7
64	Atomic Arrangements inside Ru and Os Nanoislands Spontaneously Deposited on Pt(111). Journal of Physical Chemistry B, 2006, 110, 13425-13429.	1.2	6
65	Water Electrolysis Accompanied by Side Reactions. Journal of Chemical Education, 2021, 98, 2381-2386.	1.1	6
66	X-ray micro computed tomography and efficient electrochemical recovery of lanthanides on porous carbon cylinder electrodes. Composites Part B: Engineering, 2022, 231, 109590.	5.9	6
67	Photoelectrochemical CO2 Reduction Products Over Sandwiched Hybrid Ga2O3:ZnO/Indium/ZnO Nanorods. Frontiers in Chemistry, 2022, 10, 814766.	1.8	6
68	Preoxidation of CO on Os-Modified Pt(111): A Comparison with Ru-Modified Pt(111). Langmuir, 2011, 27, 2044-2051.	1.6	5
69	Spectral holes and induced luminescence in KCl co-doped with Eu2+and Eu3+ions. Journal of Physics Condensed Matter, 2001, 13, 2835-2843.	0.7	4
70	Adlayers of Sb Irreversibly Adsorbed on Pt(111):Â An Electrochemical Scanning Tunneling Microscopy Study. Journal of Physical Chemistry B, 2006, 110, 10814-10821.	1.2	4
71	Electron transfer behavior at polyoxometalate-adsorbed alkanethiol self-assembled monolayers. Applied Surface Science, 2011, 257, 9490-9497.	3.1	4
72	Solution phase post-modification of a trimesic acid network on Au(111) with Zn ²⁺ ions. Chemical Communications, 2015, 51, 873-876.	2.2	4

CHOONG KYUN RHEE

#	Article	IF	CITATIONS
73	Photoluminescence imaging of europium (III)â€doped γ â€Al 2 O 3 nanofiber structures. Luminescence, 2019, 34, 838-845.	1.5	4
74	Enhanced Photoluminescence of Electrodeposited Europium Complex on Bare and Terpyridine-Functionalized Porous Si Surfaces. Photochem, 2021, 1, 38-52.	1.3	4
75	Pt Deposits on Bi-Modified Pt Electrodes of Nanoparticle and Disk: A Contrasting Behavior of Formic Acid Oxidation. Journal of Electrochemical Science and Technology, 2021, 12, 323-329.	0.9	4
76	Formic Acid Oxidation Depending on Rotating Speed of Smooth Pt Disk Electrode. Journal of Electrochemical Science and Technology, 2014, 5, 82-86.	0.9	4
77	A Contoured Network of Anionic Trimesic Acids on Au(111) and Its Host–Guest Chemistry. Journal of Physical Chemistry C, 2013, 117, 22636-22643.	1.5	3
78	Co-deposits of Pt and Bi on Au disk toward formic acid oxidation. Journal of Solid State Electrochemistry, 2020, 24, 2535-2542.	1.2	3
79	Photocatalytic and Electrocatalytic Properties of Cu-Loaded ZIF-67-Derivatized Bean Sprout-Like Co-TiO2/Ti Nanostructures. Nanomaterials, 2021, 11, 1904.	1.9	3
80	Multiple Nonenzymatic Labels-Based Impedimetric Aptamer Sensor for the Competitive Detection of Thrombin. Bulletin of the Korean Chemical Society, 2013, 34, 721-722.	1.0	3
81	Electrochemical Ce(III)/Ce(IV) interconversion, electrodeposition, and catalytic COÂ↔ÂCO2 interconversion over terpyridine-modified indium tin oxide electrodes. Journal of Industrial and Engineering Chemistry, 2022, 106, 520-536.	2.9	3
82	Adsorptive Behavior of Dimethylglyoxime on Au(111). Langmuir, 2011, 27, 14638-14646.	1.6	2
83	Electrochemical behaviors and electrodeposited materials of lanthanides (La, Ce, Pr, Nd, Sm, Eu, Gd, Tb,) Tj ETQq 27, 102305.	l 1 0.7843 0.9	14 rgBT /Ovo 2
84	Electrochemistry, Electrodeposition, and Photoluminescence of Eu (III)/Lanthanides (III) on Terpyridine-Functionalized Ti Nanospikes. Metals, 2021, 11, 977.	1.0	2
85	PT-BI Co-Deposit Shell on AU Nanoparticle Core: High Performance and Long Durability for Formic Acid Oxidation. Catalysts, 2021, 11, 1049.	1.6	2
86	Photodissolution of cleaved CdTe(110): atomic force microscopic and Auger electron spectroscopic study. Applied Surface Science, 2002, 187, 179-186.	3.1	1
87	Spontaneous Deposition of Ultrathin Ag Shell on Cu Nanoparticle Core Using Galvanic Replacement. Bulletin of the Korean Chemical Society, 2016, 37, 258-261.	1.0	1
88	Structural evolution of trimesic acid (TMA)/Zn 2+ ion network on Au(111) to final structure of (10â^š3 ×) Tj ETC	2q0.8 0 rg	BT /Overlock
<u> 00-</u>	Electrochemical Cr(VI) Reduction over Terpyridine-Derivatized Ti Sheets. Applied Science and	0.2	0